International Journal of Pharmaceutics 695 (2026) 126745

Contents lists available at ScienceDirect

International Journal of Pharmaceutics

journal homepage: www.elsevier.com/locate/ijpharm

Enhanced transdermal delivery of [6]-Gingerol via Co-Administration of Acmella oleracea and *Zingiber officinale* lipophilic extracts☆

Greta Camilla Magnano [a,b,*], Martina Glerean [a], Stefano Dall'Acqua [c], Michela Abrami [d], Francesca Larese Filon [b], Flavia Carton [e,f,g], Manuela Malatesta [e], Laura Calderan [e], Andrea Galvan [e,h], Dario Voinovich [a], Dritan Hasa [a,*]

[a] Department of Chemical and Pharmaceutical Sciences, University of Trieste, Italy
[b] Clinical Unit of Occupational Medicine, University of Trieste, Italy
[c] Department of Pharmaceutical Science and Pharmacology, University of Padova, Italy
[d] Department of Engineering and Architecture, University of Trieste, Italy
[e] Department of Neurosciences, Biomedicine and Movement Sciences, University of Verona, Italy
[f] Interdepartmental Center of Medical Sciences (CISMED), University of Trento, Italy
[g] Department of Cellular, Computational and Integrative Biology (CIBIO), University of Trento, Italy
[h] Department of Diagnostics and Public Health, University of Verona, Italy

ARTICLE INFO

Keywords:
Zingiber officinale
Acmella oleracea
[6]-gingerol
Spilanthol
Natural products
Galenic formulation

ABSTRACT

Acmella oleracea and Zingiber officinale (ginger) are two plants of great interest due to their antioxidant, antimicrobial, and especially anti-inflammatory properties. These effects are mainly attributed to the presence of bioactive compounds such as spilanthol in Acmella oleracea and [6]-gingerol in Zingiber officinale. However, [6]-gingerol is primarily metabolised at the gastrointestinal and hepatic levels after oral administration, limiting its systemic bioavailability and effectiveness. In this study, a cream formulation containing both extracts was prepared using a preformed commercial transdermal vehicle and characterised through rheological studies. The ex vivo skin permeation of spilanthol and [6]-gingerol was evaluated using Franz diffusion cells. Results showed that the presence of Acmella oleracea lipophilic extract promoted the permeation of [6]-gingerol. Moreover, no histological alterations were observed in explanted human skin after transdermal application in a fluidic dynamic system. Based on these findings, topical administration of a formulation containing both Zingiber officinale and Acmella oleracea lipophilic extracts appears to be a promising strategy for enhancing the skin permeability of the active ingredients and, specifically for [6]-gingerol, avoiding its transformation in the gastrointestinal tract.

1. Introduction

Acmella oleracea also known as Spilanthus oleracea possesses various beneficial properties including anaesthetic, anti-inflammatory and antioxidant activities (Rondanelli, 2020), with its main active compound spilanthol being effective *in vitro* at concentrations of 3–100 μM (Abdul, 2021; Huang et al., 2018). This plant is particularly rich in alkaloids such as n-alkylamides, as well as stigmasterol and triterpenoids, and amino acids. Specifically, spilanthol, an aliphatic amide with an isobutyl side chain is the most abundant N-alkylamides. which exhibits analgesic, diuretic, fungistatic, bacteriostatic activities (Ratnasooriya et al., 2004; Molina-Torres et al., 2004; Rios and Aguilar-Guadarrama, 2007), and has been used also for the treatment of eczema (Boonen et al., 2010). The anti-inflammatory activity of spilanthol is attributed to the inhibition of the JNK (c-Jun N-terminal kinase) signaling pathway. Additionally, this molecule reduces the production of pro-inflammatory mediators induced by TNF-α (tumor necrosis factor- α), downregulate ICAM-1(intercellular adhesion molecule-1), and the expression of cyclooxygenase-2, while it promotes the HO-1(heme oxygenase-1) expression (Huang et al., 2018). Similarly, ginger (*Zingiber officinale*) exhibits several biological activities, such as anti-inflammatory, antioxidant, antimicrobial, antiallergic and antitumor effects. These characteristics are mainly attributed to the presence of gingerols, particularly [6]-gingerol, and to its dehydrated version (shogaol) (Rios

☆ This article is part of a special issue entitled: 'Joke Bouwstra_IJP' published in International Journal of Pharmaceutics.

* Corresponding authors.
E-mail addresses: gmagnano@units.it (G.C. Magnano), dhasa@units.it (D. Hasa).

https://doi.org/10.1016/j.ijpharm.2026.126745
Received 16 September 2025; Received in revised form 23 February 2026; Accepted 2 March 2026
Available online 10 March 2026

and Aguilar-Guadarrama, 2007; Semwal et al., 2015)-gingerol which also imparts characteristic pungency of ginger. Importantly, [6]-gingerol undergoes extensive GI and hepatic metabolism when administered orally, which may reduce its bioavailability and therapeutic effectiveness (Arcusa et al., 2022). In this study, we decided to bypass first-pass metabolism and explore the transdermal route of such active ingredient. This approach may enhance the local availability of [6]-gingerol at the site of action, potentially amplifying its anti-inflammatory effects. Based on the established analgesic and anti-inflammatory properties of both spilanthol and [6]-gingerol, the topical formulations investigated in this study are intended for targeted management of localized inflammation. Moreover, both spilanthol and [6]-gingerol have physico-chemical properties suitable for absorption across the skin, including a moderate solubility in oil and water, a partition coefficient (log P) ranging from 2.5 to 3.8, and a molecular weight under 500 Da. Spilanthol has a log P of approximately 3.4 (Boonen et al., 2010); while [6]-gingerol has a log P in the range 2.8–3.5 (Minghetti et al., 2007), supporting their preferential affinity for lipid-rich domains of the *stratum corneum*. According to the extensive work of Bouwstra and co-workers, the *stratum corneum* lipid matrix is organised in highly ordered lamellar structures that represent the main pathway and barrier for transdermal transport (Bouwstra et al., 2023; Uche et al., 2021; Uche et al., 2019; Bouwstra, 2003). Their studies demonstrated that small and moderately lipophilic molecules preferentially diffuse through the intercellular lipid domains and that alterations in lipid packing and fluidity can significantly enhance skin permeability. In this context, penetration enhancers are known to act by increasing lipid mobility and creating transient pathways for drug diffusion. Based on these fundamental concepts, we speculate that spilanthol, can interact with *stratum corneum* lipids, therefore acting as a penetration enhancer for [6]-gingerol. These two plants (*Acmella oleracea* and *Zingiber officinale*) are currently combined in a commercial formulation of the two standardised botanical extracts for an oral administration available in capsules and tablets, acting as natural adjuvant for ache management (Rondanelli et al. 2020). Moreover, such association has been shown promising effects in cosmetic applications, in particular in the aging process by improving the dermal density (Moldovan et al., 2016). Although some nanocarrier systems for both [6]-gingerol and spilanthol have been explored, these approaches often involve complex preparation, high surfactant content and limited scalability. For this reason, Pentravan® was selected as a commercially standardised, dermatologically validated transdermal base, widely used in compounding practice, offering high reproducibility and favourable patient compatibility as a practical vehicle for incorporating both botanical extracts. Considering the current lack of effective formulations, the cutaneous application of a cream containing both *Acmella oleracea* and *Zingiber officinale* lipophilic extracts appears to be a promising alternative for the simultaneous delivery of spilanthol and [6]-gingerol. The current work aimed to investigate the transdermal behaviour of a novel formulation obtained by combining *Zingiber officinale* and *Acmella oleracea* lipophilic extracts, therefore focusing on the simultaneous delivery and potential synergistic effects of [6]-gingerol and spilanthol. The two extracts were combined in a 1:1 weight/weight (w/w) ratio in order to ensure a balanced contribution of both active components, maximising the potential for synergistic anti-inflammatory and analgesic effects. Specifically, we explored the possibility of spilanthol acting as a skin penetration enhancer for [6]-gingerol. To further support such hypothesis, we also evaluated the permeability of a cream containing only *Zingiber officinale* as a control product. *In vitro* permeation experiments were conducted using Franz diffusion cells, and the amount of actives in different skin layers was quantified. The quantitative analysis of *stratum corneum* distribution via tape stripping enabled assessing the depth-dependent accumulation of both actives and to provide experimental evidence of the synergistic effect between the actives. Additionally, the biocompatibility and tissue-level impact of the formulations were evaluated on explanted human skin using a dynamic perfusion bioreactor system, offering a physiologically relevant model to assess potential structural alterations.

2. Material and methods

2.1. Materials

In the current research work, *Zingiber officinale* lipophilic extract and *Acmella oleracea* lipophilic extract were purchased from Indena S.p.a, (Italy). The transdermal vehicle (commercial name Pentravan®) was obtained from Fagron Italia S.r.l. Acetone and ethanol (EtOH) used for analytical purposes were both of HPLC grade, and were purchased from Sigma-Aldrich (St. Louis, USA). Potassium dihydrogenphosphate, sodium chloride and sodium hydrogenphosphate were obtained from Carlo Erba (Italy). A Millipore purification pack system was used to produce MilliQ water. The physiological solution was prepared by dissolving 9 g of NaCl, 0.19 g of KH_2PO_4, and 2.38 g of Na_2HPO_4 1 L of MilliQ water, with a final pH of 7.35. Base formulation with hydrogenated phosphatidylcholine and skin identical lipids of the *stratum corneum* SLM (Skin Lipid Matrix®), Lipoid GmbH, Germany.

2.2. Lipophilic extracts standardisation

The lipophilic extracts of *Zingiber officinale* and *Acmella oleracea* were kindly provided by Indena S.p.A. (Milan, Italy). Both extracts are obtained using supercritical CO_2 extraction. To verify extract composition and ensure standardisation, we performed Liquid Chromatography with Diode Array Detection and Mass Spectrometry (LC-DAD-MS) analysis using an Agilent 12,560 LC system equipped with a diode array detector (DAD) and coupled to a Varian MS 500 mass spectrometer operating with an electrospray ionisation (ESI) source. Chromatographic separation was achieved with an Eclipse XDB C18 column (3 × 150 mm, 3.5 μm). The mobile phases were (A) water containing 1% formic acid and (B) acetonitrile. The flow rate was 300 μL/min and the gradient elution profile started with 70% A and kept isocratic for 14 min. It then reached 100% B after 10 min and kept isocratic for 14 min. The post-column flow was split equally between the DAD and MS detectors. Mass spectra were acquired in both positive and negative ion modes. The scan range was *m/z* 100–1500 in negative mode and *m/z* 100–1100 in positive mode. Physical characterisation of the extracts, including viscosity and density, was also performed.

2.3. Solubility of actives from lipophilic extracts

The equilibrium solubility for both *Zingiber officinale* and *Acmella oleracea* extracts was measured following a method already reported in the literature with minor modifications (Matchimabura et al., 2024), using a shake-flask approach (Kerdsakundee et al., 2015). Briefly, 1.0 mL of phosphate-buffered saline (PBS, pH 7.4) was introduced into a glass vial, followed by the addition of an excess amount of the extract. The samples were initially mixed using a vortex mixer for 10 min to promote dispersion and then incubated in a thermostated shaking water bath at 32 ± 0.1 °C under continuous agitation (100 rpm). After 72 h, the suspensions were centrifuged at 6000 rpm for 20 min, and the resulting supernatants were collected and filtered through 0.45 μm membrane filters. The concentrations of [6]-gingerol and spilanthol were subsequently quantified by HPLC–MS analysis, as described in Section 2.2. For each extract the solubility experiments were carried out in triplicate.

2.4. Preparation of topical creams

The two topical formulations were prepared by mechanical incorporation of the natural extracts, i.e. *Zingiber officinale* and *Acmella oleracea* into a preformed transdermal oil-in-water vehicle, which was selected based on our previous work with another active ingredient

(Magnano, 2024). Specifically, formulation A was prepared by mechanical incorporation of *Zingiber officinale*, while formulation B included both *Zingiber officinale* and *Acmella oleracea* extracts. The concentration of *Zingiber officinale* extract in formulation A was selected based on published literature reporting topical formulations containing approximately 20% (w/w) ginger extract (Novianti, 2022) to elicit measurable biological effects. Hence, a total extract load of 25% (w/w) was therefore chosen for formulation A and kept constant in formulation B by dividing the total amount into 12.5% (w/w) *Zingiber officinale* and 12.5% (w/w) *Acmella oleracea*. Macroscopically, both formulations appeared homogeneous and free of visible phase separation. Formulation A showed a mustard-yellow color, whereas formulation B exhibited a caramel-brown color. Table 1 shows the final composition of the two creams including the content of actives (% w/w). The ingredients of the oil-in-water base are listed as follows: isopropyl myristate, PEG-40 stearate, EDTA, glyceryl monostearate, butylated hydroxytoluene, urea, stearyl alcohol, isopropyl palmitate, carbomer, potassium sorbate, stearic acid, lecithin, cetyl alcohol, sorbic acid, simethicone, hydrochloric acid, benzoic acid, water. The transdermal vehicle is a commercially available formulation. The manufacturer provides only a qualitative list of ingredients. The products were stored at room temperature for less than 24 h, prior the assessment of the absorption study. To determine the effective concentration of [6]-gingerol and spilanthol in each formulation, 30 mg of either formulation A or formulation B were dispersed in 6.0 mL of water/EtOH solution 50/50% (v/v). The samples were sonicated for 30 min and subsequently centrifuged for 10 min (1000 rpm, 25°C). Eventually, 1.0 mL of the supernatant was collected, filtered, and quantified using UV-HPLC (see paragraph 2.10). The extraction method was further verified by measuring the [6]-gingerol content at 6 h, 24 h, 48 h, and 1 week after formulation preparation. Consistent amounts were observed at all time points, confirming the reliability of the extraction procedure and the stability of the active compounds in the formulations.

2.5. Rheological analysis

The Haake Mars Rheometer was used to evaluate the rheological features of the two formulations. This stress controlled rotational rheometer was provided with a Peltier temperature control system and plate-plate geometry PP60 with a diameter of 60 mm. Creams were loaded between the two plates and a fixed gap of 0.3 mm was adopted for all measurements. Two different analyses were performed to determine the viscoelastic features of the creams. Flow experiments were conducted at fixed temperature of 37 °C, with shear ranging from 0.1 to 100 Pa. Mechanical spectra were determined at constant temperature (37 °C) and shear stress (0.5 Pa), with a sweep of frequency between 0.1 and 100 Hz.

2.6. In vitro release test of actives from topical formulations

The *in vitro* release of the active compounds from the tested formulations was evaluated using vertical Franz-type diffusion cells (diffusion area: 3.14 cm^2; receptor volume: 15 mL), equipped with synthetic PermeaPlain® barriers (Phabioc InnoME GmbH, Espelkamp, Germany), which were used as the release barrier. The membranes were set between the donor and receptor compartments, with the active side facing the donor phase. An accurately weighed amount of 31.4 mg for each formulation (the experimental amount of the actives in each cream is shown in paragraph 2.3) was applied to the donor compartment, while the receptor compartment was filled with receptor medium: water/EtOH solution (50/50 %v/v), continuously stirred with a magnetic bar at 500 rpm and thermostated at 32 ± 0.5 °C to mimic skin surface conditions. At predetermined time intervals (0, 0.5, 1, 2, 3, 4, 5, and 6 h), 1.0 mL aliquots were withdrawn from the receptor phase and replaced with fresh preheated medium to maintain sink conditions. The collected samples were analysed by HPLC (see section 2.10). All experiments were performed in triplicate, and the results were expressed as the cumulative percentage (%) of the total active content in the formulation versus time. Coefficients of determination R^2 were calculated and those with a value higher than 0.99 were considered linear.

Table 1
Formulation composition (% w/w), experimental amounts of actives and transdermal vehicle.

FORMULATION	Amount of transdermal vehicle (% w/w)	Amount of lipophilic extract (% w/w)	
		[6]-gingerol	spilantol
Formulation A	75	25	/
Formulation B	75	12.5	12.5

2.7. Preparation of porcine ear skin

Porcine skin, due to its comparable permeability and morphology to human skin, was selected as a model to assess penetration experiments (Barbero and Frasch, 2009; Simon and Maibach. 2000; Schmook et al., 2001; Wester et al., 1998). Pig skin samples were sourced from animals already slaughtered for the food industry; therefore the ethical approval was not required. Ear from piglets were collected and preserved at −25 °C for two months. Before performing the test, a physiological solution was used to thaw the skin for preventing dehydration and maintaining a physiological pH during thawing, as also described in our previous study (Magnano et al., 2022). The skin samples were cut into 5 cm^2 square pieces and the thickness was determined using a micrometric caliper (Mitutoyo), achieving a mean value of 1.00 ± 0.03 mm. The observed thickness is in accordance with OECD Test Guideline 428 (Guidance Document For The Conduct Of Skin Absorption Studies Oecd Series On Testing And Assessment Number 28, 2004), which recommends the use of skin with a thickness not exceeding about 1 mm for *in vitro* dermal absorption assays. After one hour of equilibration, on each skin piece, it was measured the trans epidermal water loss (TEWL) in order to measure skin integrity. The measurements were carried using a vapometer (Delfin Vapometer) previously utilized in our studies (Magnano, 2024; Magnano et al., 2022) and the samples had TEWL values less than 10 $g \cdot m^{-2} \cdot h^{-1}$ (Guth et al., 2015).

2.8. In-vitro penetration assay

2.8.1. Retention and permeation profile of actives from topical formulations

According to the OECD guidelines for the testing of molecules (OECD, 2004); (Guidance Document For The Conduct Of Skin Absorption Studies Oecd Series On Testing And Assessment Number 28, 2004) cutaneous absorption assays were conducted with Franz-type static diffusion cells. The skin tissue was placed between the receptor and donor compartments, with the *stratum corneum* facing the donor compartment. The total skin area exposed was 3.14 cm^2. The receptor chamber (RC) possess a volume of 15 mL and was filled with receptor fluid (RF), consisting of phosphate buffered saline (PBS, pH 7.4). The receptor medium was continuously stirred under magnetic agitation to ensure homogeneity. This receptor fluid was selected to ensure biocompatibility with the skin and adequate solubility of both actives, in line with PBS-based receptor media reported for [6]-gingerol (Intawong et al., 2025) and spilanthol (Boonen et al., 2010). The temperature of the water bath was 32 ± 1 °C. At the beginning of the experiment (time 0), 31.4 mg of each cream was directly deposited on the surface of the skin and thanks to a cotton swab with a gloved finger it was spread on the skin surface as homogenously as possible. This corresponded to a theoretical applied dose (Q_0) of 10.0 mg/cm^2, calculated as 31.4 mg applied over 3.14 cm. Such finite dose was chosen to reflect realistic topical application conditions, as recommended in OECD guidelines (OECD, 2004), allowing evaluation of absorption and retention of the

actives in the skin layers under clinically relevant conditions. To ensure accurate dose application, each cream sample was weighed before and after application. The cotton swab, used exclusively to ensure homogeneous spreading of the formulation, was also weighed before and after use; the retained amount was consistently about 1.2 ± 0.03% of the applied dose. To evaluate the permeation profile of spilanthol and [6]-gingerol retaining and diffusing into the layers of the skin, the permeation assay lasted 24 h. Samples of the RF were collected at time 0, 1, 2, 3, 4, 5, 6, and 24 h. Sink conditions, throughout the 24-hour experiment, were maintained by replacing immediately with the same volume of fresh medium, continuously stirred. Experiments were performed in six replicates. Skin from at least 3 distinct pigs was adopted. The contents of actives registered in RF and in the layers of skin were determined using HPLC (section 2.10) at the end of the experiment. At the end of the experiment, a full mass-balance approach was applied to validate the extraction procedure. The cumulative amount permeated into the receptor fluid, the amount retained in the *stratum corneum*, the amount retained in the viable epidermis/dermis, and the residue recovered during the cleaning step were quantified and summed. Recovery (%) was calculated as the ratio between the total recovered amount and the applied dose.

$$\text{Recovery}\ (\%) = \frac{\text{total recovered amount}}{\text{applied dose}} \text{x}\,100$$

2.9. Samples collection

After the contact time (24 h), all cells are dismantled. Then, the RF was collected and stored at −20 °C. The donor chamber, defined as the fraction non-absorbed from the skin, was washed using MilliQ water (3.0 mL). The washing solution was transferred into a Falcon tube with 6.0 mL of ethanol (EtOH). The skin membranes having an area of 3.14 cm^2 were cut in "little circles". From viable layers, the total *stratum corneum* (SC) was separated using tape stripping technique (7 strips) with D-Squame tape and transferred with 5.0 mL of EtOH in a vial under stirring for 4 h. Each strip was weighed individually using an analytical balance (N = 3). To better investigate the potential synergistic effect between the active compounds, each strip was also processed separately by immersing in 2.0 mL of EtOH. The immersed strip was subsequently stirred for 4 h, filtered, and analysed by LC-DAD-MS, as described in Section 2.2. The amount of active compound recovered from each strip was normalised to its weight. Normalisation by strip weight accounts for any variations in the amount of *stratum corneum* collected. The D-Squame tapes used in this study are standardised discs, ensuring consistent thickness and adhesive properties for each strip, making the normalisation a reliable approach for quantitative comparison between samples. Then, a scalpel was used to cut into small pieces the epidermis and dermis (E + D) layers which are mixed with solvent (2.0 mL of EtOH), stirred for a period of time of 4 h, and subsequently diluted in EtOH (1:10) prior to UV-HPLC quantification. [6]-gingerol and spilanthol were extracted from skin layers (*stratum corneum*, epidermis + dermis) for 4 h under agitation at room temperature. Then, 1.0 mL of aliquots were filtered before UV-HPLC analysis. The experiments were performed in six replicates.

2.10. Quantification of actives by HPLC

[6]-gingerol content registered in samples were determined by UV-HPLC analysis as previously reported in our recent work (Magnano et al., 2022). For the determination of spilanthol concentrations, it was adopted an Agilent 1260 chromatograph with a diode array (Santa Clara, USA). The quantification was performed using an Poroshell 120 C18 column as stationary phase with a length of 4.6 × 250 mm and the size of particle was 5 μm (Agilent InfinityLab). The column temperature was 23 °C, while the mobile phase was 0.1% formic acid water and acetonitrile (90:10, v/v) with 0.85 mL/min as flow rate. 10 μL was the volume injection, and the wavelength detection was 254 nm. The LOD (limit of detection) and LOQ (limit of quantification) are 0.6 μg/mL and 1.4 μg/mL, respectively.

2.11. Calculations of permeability

The flux (J) was calculated according to Eq. (1).

$$J = \frac{\text{dQ}}{\text{A*dt}} \tag{1}$$

where (dQ,) is the cumulative contents of actives (expressed in μg) permeated through the membrane divided by the time (dt expressed in h) and the membrane surface area (A expressed in cm^2). Since finite dose conditions were applied, true steady-state conditions were not achieved; therefore, J represents a time-averaged permeation rate derived from the cumulative permeation profile.

The P_{app} (apparent permeability coefficient) expressed in (cm/s), under finite dose conditions, was then derived from the ratio of calculated flux J (μg/cm^2*s) to the active concentration C_d (μg/cm^3), registered in the donor compartment at the beginning of the experiment (t = 0), according to Eq. (2) and as described in the literature (Lehman and Simplified Approach, 2014).

$$P_{app} = \frac{J}{C_d} \tag{2}$$

Additionally, the Q_{abs} (total absorbed and recovered amount) was determined using Eq. (3).

$$Q_{abs} = SC + (E + D) + RC \tag{3}$$

where SC represents the total recovered amount of active compounds obtained in the *stratum corneum*, E + D refers to the total recovered amounts registered in the epidermis and dermis, and RC denotes the recovered amounts in the receptor compartment after 24 h of exposure.

2.12. Differential scanning calorimetry (DSC) analyses

Calorimetric analyses on the pure biomimetic lipid system (SLM), transdermal vehicle Pentravan®, formulation A and B, were performed on a Mettler Toledo DSC 3 instrument. In a typical experiment, about 6.0 mg of material were weighed in a 40 μ L aluminum pan and covered with an aluminium lid. After a series of preliminary trials and based on literature data (Goh et al., 2022), the samples were heated nitrogen flow (50 ml/min) from 20 °C to 100 °C, using a heating rate of 1 °C min^{-1}. The DSC curves were processed using the Mettler STARe data evaluation software (version 16.40).

2.13. Histological evaluation on human skin explants

In order to reveal possible morphological signs of the passage of actives passage through the skin, a histological analysis of human skin explants was conducted. Human skin samples were obtained as waste materials after abdominoplasty surgery carried out on a female patient. The study was conducted in accordance with the Declaration of Helsinki, and approved by the Institutional Ethics Committee of the Verona University Hospital (protocol code 3449CESC, 21 April 2021). Freshly excised explants were rapidly washed in sterile physiological solution (0.9% w/v NaCl) at room temperature and then in a pre-warmed maintenance culture medium composed of DMEM (Dulbecco's Modified Eagles's medium) supplemented with 4.5 g/L of D-Glucose, 10% v/v of FBS (Fetal Bovine Serum), 1% v/v of penicillin- streptomycin, 1% v/v L-glutamine and 0.5% w/v amphotericin B (ThermoFisher Scientific Inc., Waltham, MA, USA). The subcutaneous fatty tissue was removed, and roundish samples with a diameter of 1.5 cm were mounted inside the bioreactor chambers with the *stratum corneum* facing upwards with air and the dermis facing downwards with medium, reproducing the air-

liquid interface (IV-Tech, Massarosa, Lucca, Italy). This innovative fluidic dynamic system proved to ameliorate the structural and functional preservation of tissue explants, which maintain *in vitro* the capability to react similarly to living organs (Galvan et al. 2023; Calderan, 2022; Cappellozza et al., 2022; Cappellozza et al., 2021; Esposito et al., 2022). Using a cotton bud, 10 mg/cm^2 of the different formulations were applied on the skin surface and pre-warmed maintenance medium was placed in contact with dermis in bioreactor chambers connected in parallel with a peristaltic pump that delivers a continuous and constant flow of medium at a rate of 500 μL/min. The bioreactor was placed in an incubator, at 37 °C and 5% CO_2 humidified atmosphere for 6 h. As controls untreated skin explants were fixed either immediately after removal (CTR T0, n = 3) or after 6 h in the bioreactor (CTRB, n = 3). Skin samples were collected after 6 h of incubation based on the results of the permeation profile, which identified this time point as a meaningful and representative phase of the transdermal transport process. For histological analysis, skin explants were fixed overnight with 4% (v/v) paraformaldehyde in 0.1 M phosphate buffer at room temperature, dehydrated in ethanol, treated with xylene, and finally embedded in paraffin wax. Cross sections containing both epithelial and dermal layers were cut and stained with Mayer's hematoxylin and eosin solution (BioOptica, Italy) and observed using an Olympus microscope equipped with an Olympus Camedia 5050 digital camera (Olympus, Italy).

2.14. Statistical analysis

From skin absorption tests, data obtained are reported as mean ± standard error of the mean (SEM). Differences between two groups were assessed using the Wilcoxon–Mann–Whitney test, with a significance threshold set at $p = 0.05$.

3. Results

3.1. Characterisation of lipophilic extracts

The chemical composition of *Zingiber officinale* and *Acmella oleracea* was confirmed by LC-DAD-MS analysis as described in the Materials and Methods section. The *Zingiber officinale* extract contained 22% (w/w) [6]-gingerol, while the *Acmella oleracea* extract contained 16% (w/w) spilanthol, consistent with the specifications reported by the respective manufacturer. The [6]-gingerol and the spilanthol can be detected in the diode array, as represented in Fig. 1S (Supplementary Information) and are also confirmed by their MS data obtained in positive and negative mode respectively at retention time (rt) of 13.6 min (*m/z* 222 in positive mode) and 11.7 min. In Fig. 1 is reported a typical chromatogram of the

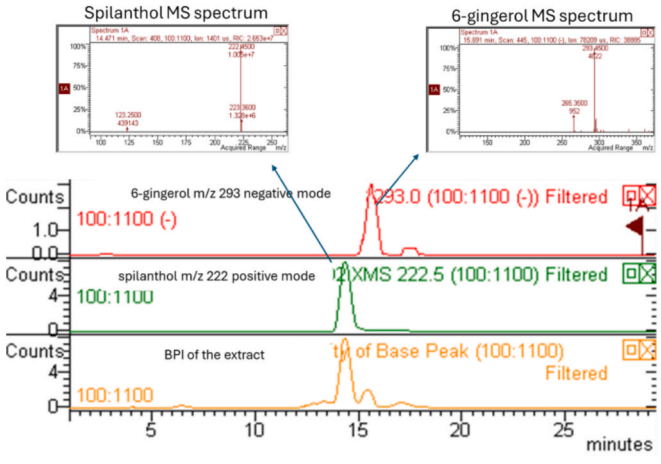

Fig. 1. The chromatograms for spilanthol and [6]-gingerol respectively as well as their MS spectrum.

standardised *Zingiber officinale* and *Acmella oleracea* extract, including the Base Peak Intensity (BPI), which represents the most intense ion detected at each retention time throughout the LC-MS run. Additionally, the figure includes the extracted ion chromatograms (EIC) for the two compounds, spilanthol and [6]-gingerol, which were selectively monitored based on their specific mass-to-charge (*m/z*) values. The respective MS spectra of two active molecules are also illustrated in the Fig. 1. In addition to chemical standardisation, the physical properties of the lipophilic extracts were evaluated. The *Zingiber officinale* extract showed a viscosity of 0.25 Pa·s, and a density of 1.22 g/mL, whereas the *Acmella oleracea* extract exhibited a viscosity of 0.80 Pa·s, and a density of 1.43 g/mL.

3.2. Cream formulations characterisation, rheological analysis and release kinetics

The stability of both formulations was evaluated over a 30-day period, which is consistent with the typical shelf-life of extemporaneous galenic preparations. The formulations were prepared following the procedure described in the Materials and Methods section and were stored in closed containers at room temperature (20–25 °C) protected from light. No phase separation or syneresis was observed. Moreover, the contents of [6]-gingerol and spilanthol in the formulations did not change after 30 days, indicating that no degradation effect occurs during the time. At time zero, the experimental amounts of [6]-gingerol were 3.43 ± 0.04 mg for formulation A and 1.76 ± 0.06 mg for formulation B. Additionally, formulation B contained 1.05 ± 0.01 mg of spilanthol. After 30 days, the measured contents [6]-gingerol were 3.42 ± 0.09 mg for formulation A; 1.78 ± 0.03 mg and for formulation B and 1.06 ± 0.04 mg of spilanthol contained in formulation B, confirming the stability of both compounds in the creams over the tested period. The rheological behaviour of the two topical formulations is reported in Fig. 2. In Fig. 2 (I) are reported the flow curves: for both formulations there were a first stage of stable viscosity followed by a rapidly decreased after the overtaken of critical threshold of shear stress/rate, ending with a second viscosity plateau. This represents a typical shear thinning behaviour, a desired condition for cream preparation: at the application time, cream stays without trickling, consumers should apply a force to spread the cream reducing its viscosity and allowing skin penetration. Formulation A (containing only the *Zingiber officinale* lipophilic extract) exhibited slightly higher viscosity compared to formulation B (containing both *Zingiber officinale* and *Acmella Oleracea* lipophilic extracts).

Viscosity data from a shear thinning material, could be correlated with good approximation with the Cross model equation (Cross, 1965) to obtain the so called zero shear rate viscosity, η_0.

$$\eta = \eta_\infty + \frac{\eta_0 - \eta_\infty}{1 + (\lambda\dot{\gamma})^n} \tag{4}$$

where η_0 and η_∞ are the asymptotic values of the viscosity at zero and infinite shear rates, respectively, λ is the characteristic time, $\dot{\gamma}$ is the shear rate and n measures the shear rate dependence of viscosity in the power law region. The calculated η_0 reported in Table 2, indicate sample A as the more viscous formulation.

The frequency sweep plot in Fig. 2II shows the so-called mechanical spectra: elastic and viscous moduli (G' and G'' respectively) in function of frequency, f. Based on this data, G' and G″ exhibited frequency-dependent behaviour, with both parameters rising as frequency increased. Furthermore, across all frequencies, G' surpassed G″, evidenced substantially a prevalent elastic property (Razi et al., 2020). Hence, these formulations did not show a liquid behaviour (where G''> G'), but the dependence of G' on frequency underlying the softness of the creams, the behaviour of the two products ressembled more to a weak gel. Formulation A exhibited higher G' and G'' in the area of high frequency, where the elastic properties are enhanced, while in the low

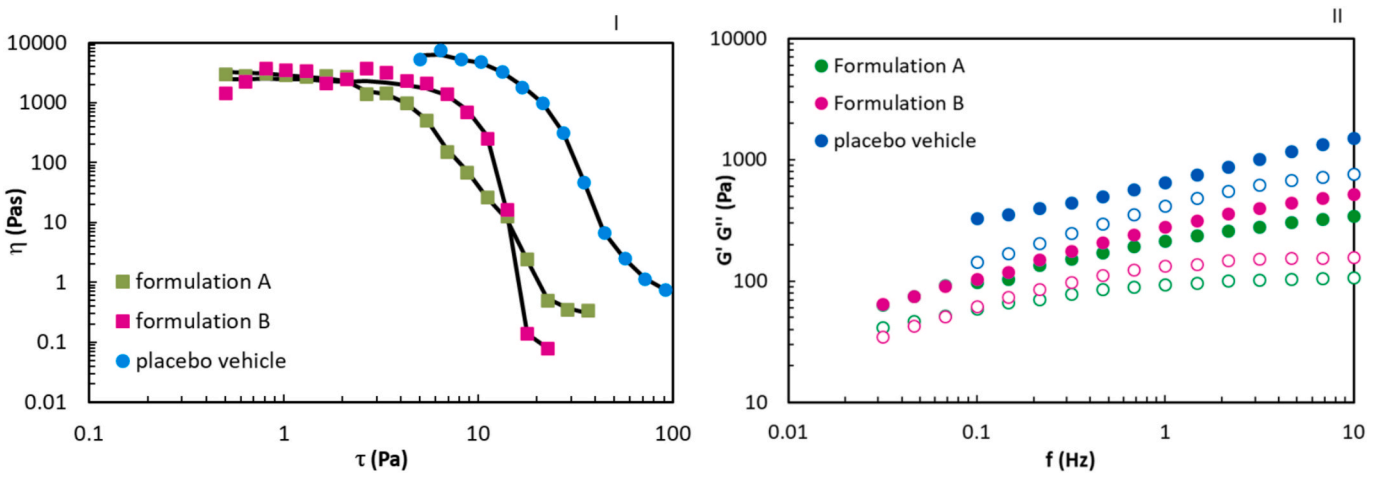

Fig. 2. Rheological tests on formulations A (green), B (pink) and placebo vehicle (blue). Flow curve (I): viscosity, η, ongoing with shear stress, τ. Black lines represent the fitting with the Cross'-model Frequency sweep (II): G' (filled symbols), G'' (open symbols) with frequency, f.

Table 2
Values of viscosity at zero stress (η_0) of the tested cream formulations.

Formulation	Viscosity at zero stress (η_0) (Pa·s)
Formulation A	384
Formulation B	261
Placebo vehicle	937

frequency region where the viscous component acquired meaning, both formulations present same moduli. The *in vitro* release profiles of [6]-gingerol and spilanthol from the tested formulations are reported in Fig. 3.

A time-dependent increase in the cumulative release of all actives can be observed over the 6-hour experimental period. Formulation B exhibited a slightly higher release of [6]-gingerol compared to formulation A at all time points. At the end of the 6-hour period, the percentage of [6]-gingerol released reached 71.3 ± 5.7% for formulation A and 90.9 ± 3.8% for formulation B. Moreover, the amount of spilanthol released from formulation B was 56.4 ± 7.0% after 6 h. The release kinetics of [6]-gingerol appeared formulation-dependent, suggesting a strong influence of the presence of spilanthol on modifying the diffusion pathway of such compound. To better understand the release mechanisms of the active compounds, the *in vitro* release data, expressed as the percentage of drug released (%), were fitted using several kinetic models (Table 3).

All datasets showed good linearity across models. The Higuchi model, describing drug diffusion release from semi-solid formulations

Table 3
Correlation coefficients (R^2) obtained by fitting the drug release data to different kinetic models.

Active	Zero Order	First Order	Higuchi	Korsmeyer–Peppas
[6]-gingerol from Formulation A	0.776	0.957	0.993	0.980
[6]-gingerol from Formulation B	0.696	0.937	0.997	0.987
Spilanthol from Formulation B	0.807	0.895	0.995	0.984

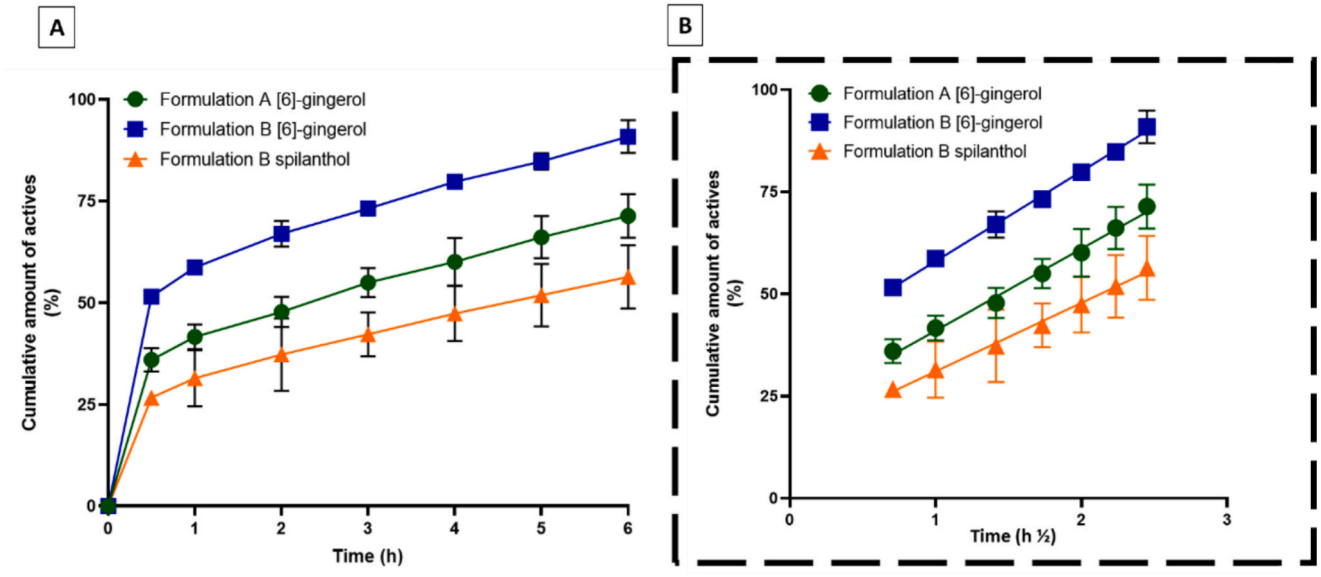

Fig. 3. A: Release test of actives from each formulation. Data are expressed as mean ± SD. Release of actives from the cream formulations is reported as the cumulative percentage (%) relative to the total content in each formulation. B: *In vitro* release data were fitted to the Higuchi model.

(Kanfer et al., 2017) (Fig. 3;Table 3), provided the best fit, with R^2 values of 0.993 for [6]-gingerol in the formulation A, 0.997 and 0.995 respectively for [6]-gingerol and for spilanthol in the formulation B, suggesting diffusion as the predominant release mechanism. Additionally, the Korsmeyer–Peppas model also showed a good fit ($R^2 = 0.98$), supporting the same mechanistic interpretation (Table 3). Notably, the release of [6]-gingerol in formulation B is higher, suggesting that spilanthol can act as a permeation enhancer through the improvement of the diffusion process.

3.3. Permeation assay of actives from cream formulations

Prior to the permeation experiments, the solubility of both actives was experimentally measured in phosphate-buffered saline (PBS, pH 7.4), according to a literature-reported method (Matchimabura et al., 2024). Under these conditions, [6]-gingerol showed a solubility of 0.62 ± 0.03 mg/mL, while spilanthol exhibited a solubility of 0.016 ± 0.0006 mg/mL in PBS. These values are consistent with literature reports indicating that [6]-gingerol has limited solubility in water (< 1 mg/mL at 25 °C) (Matchimabura et al., 2024), while spilanthol is practically insoluble in water (0.019 mg/mL) (Boonen et al., 2010). Such low aqueous solubility values for both compounds is in agreement with their lipophilic character, as showed by their reported log P values (approximately 2.5–3.8). Fig. 4 reports the amount of actives per skin area that permeated from the topical formulations into the receptor chamber. The concentration of the actives permeated through the skin increases over time. It can be clearly noticed that formulation B exhibited higher skin permeation of [6]-gingerol compared to those measured for formulation A (standard control). Indeed, the mean concentration of [6]-gingerol measured in the receptor compartment was significantly higher for formulation B than those obtained in formulation A at the end of 24 h ($p = 0.0001$) (Fig. 4). Moreover, the content of [6]-gingerol from formulation B observed in RF is higher compared to those of spilanthol from the same formulation. Furthermore, the fluxes (J) and the apparent permeability coefficients (P_{app}) were calculated for each active and reported with two significant digits (Table 4). The flux value of [6]-gingerol from formulation B was significantly higher than that observed for formulation A. As it listed in Table 4 after 24 h of exposure, the flux of spilanthol in formulation B was slightly higher than that observed for [6]-gingerol from formulation A. Moreover, formulation B showed a higher P_{app} of [6]-gingerol than that obtained from formulation A, while the P_{app} value of spilanthol in formulation B was 2.8 x 10^{-9} ± 0.15 x 10^{-9} cm/s.

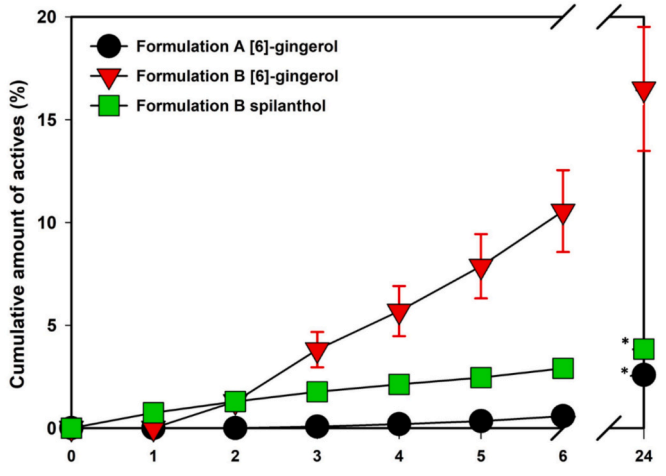

Fig. 4. Permeation profiles of actives from the tested formulations during 24 h. Data are shown as mean ± SEM (n = 6). * denotes statistically significant differences between [6]-gingerol from formulation B and [6]-gingerol from formulation A ($p = 0.0001$).

Table 4
J, P_{app} and actives concentrations obtained for each formulation tested. Data are presented as mean ± SEM (n = 6).

Active	J (μg/cm^2*s)	P_{app} (cm/s)	Actives concentration in RF at 24 h (%)
[6]-gingerol from Formulation A	0.59 x 10^{-4} ± 0.07 x 10^{-4} *	2.4 x 10^{-9} ± 0.13 x 10^{-9}	2.6 ± 0.23*
[6]-gingerol from Formulation B	1.4 x 10^{-4} ± 0.21 x 10^{-4}	4.3 x 10^{-9} ± 0.98 x 10^{-9}	16 ± 3.0
Spilanthol from Formulation B	0.78 x 10^{-4} ± 0.02 x 10^{-4}	2.8 x 10^{-9} ± 0.15 x 10^{-9}	3.8 ± 0.16

* represents statistically significant differences between [6]-gingerol from formulation B and [6]-gingerol from formulation A (Flux p = 0.0012; RF p = 0.0001).

3.4. Distribution in the skin layers of actives from cream formulations

The amount of [6]-gingerol and spilanthol from the topical creams retained by the various skin layers was also evaluated and is reported in Table 5. It can be clearly observed that the amounts of [6]-gingerol from both tested topical formulations were significantly lower in the *stratum corneum* (SC) compared to those registered in epidermis and dermis (E + D) for formulation B (Table 5). On the other hand, the contents of spilanthol accumulated in *stratum corneum* and in the other two layers such as epidermis and dermis, were found to be similar (Table 5), indicating that this active is equally distributed in these two skin layers. Furthermore, the total skin content of [6]-gingerol was significantly higher in the formulation B, which contains both extracts compared to the total skin content obtained with formulation A (Table 5). Additionally, the quantification of actives in each strip provides a clearer representation of the amount of the active ingredients accumulated per unit mass of *stratum corneum*.

As shown in Fig. 5, spilanthol exhibited higher accumulation in the uppermost SC layers (strips 1–3) compared to [6]-gingerol. This strip-by-strip analysis reinforces the hypothesis that spilanthol may act as a penetration enhancer by altering the structure of the superficial lipid domains, thus facilitating deeper diffusion of [6]-gingerol. Finally, Q_{abs} for each active was determined as reported in section 2.10 and the obtained values are listed below in Table 5. The Q_{abs} values of [6]-gingerol observed from formulation A was significantly lower than those registered for formulation B.

3.5. Thermal analysis

The thermograms of sample were reported in Fig. 6.

In order to observe possible interactions between the lipids of the *stratum corneum* and the formulation B, we used DSC since this technique shows a good sensitivity to changes in lipid organisation and phase

Table 5
Amounts of actives from the tested formulations that penetrated in the different skin layers. Data are shown as mean ± SEM (n = 6). Values in parentheses represent the coefficient of variation (CV, %).

Active	*Stratum corneum* (SC) (%)	Epidermis + Dermis (E + D) (%)	Total skin (SC + E + D) (%)	Q_{abs} (RF + SC + E + D) (%)
[6]-gingerol from formulation A	2.1 ± 0.17 (8.3) *	6.5 ± 0.43 (6.6) *	8.5 ± 0.95 (11) *	11 ± 0.84 (7.6)*
[6]-gingerol from formulation B	6.9 ± 0.59 (8.5)	14 ± 1.40 (10)	21 ± 1.5 (7.3)	37 ± 1.9 (5.0)
Spilanthol from formulation B	5.6 ± 0.38 (6.7)	6.0 ± 0.32 (5.3)	12 ± 0.68 (5.8)	15 ± 0.66 (4.2)

* denotes statistically significant differences between [6]-gingerol from formulation B and [6]-gingerol from formulation A.

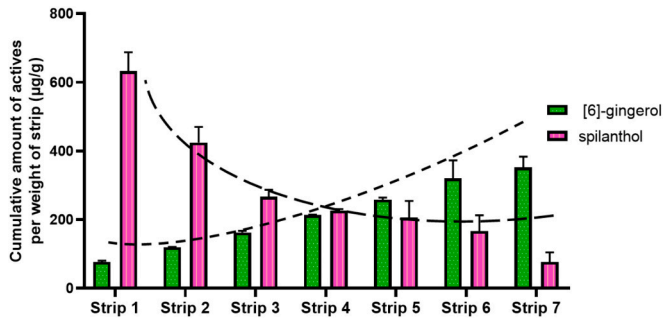

Fig. 5. Quantification of the actives from formulation B in each strip. The data was normalised by the weight of the strips. Mean ± SEM (n = 3).

behaviour (Goh et al., 2022). Although indirectly, thermal changes observed in a typical DSC experiment, can provide reliable evidence of compatibility and interaction between the cream and the skin. For such purpose, to mimic the lipid layers of the *stratum corneum* we used a commercial SLM which is characterised by ordered lamellar structures, exhibiting thermal transitions that can be readily modified upon incorporation of creams and/or active ingredients. Therefore, DSC enables detection of physical interactions and structural reorganisation within the lipid matrix without requiring chemical modification of the components.

The DSC thermogram of the transdermal vehicle (Pentravan®) (Fig. 6a) exhibits a weak endothermic transition between approximately 45 and 55 °C, possibly attributable to the reorganisation of the lipid phase within the cream matrix. The absence of sharp transitions confirms predominantly non-crystalline nature of the lipid phase within the original product. The thermal behaviour of SLM (Fig. 6b) reveals a more pronounced endothermic event in the range of 55–65 °C, possibly related to the disruption of more ordered structures deriving from lipid chains within the lamellar matrix of the product. The addition of 30 wt% of transdermal vehicle (Pentravan®) to the SLM (Fig. 6c) causes a partial broadening of the thermal transitions observed for the pure SLM, suggesting a physical interaction and partial miscibility between the transdermal vehicle lipids and the SLM, which possibly results in reorganisation of the lamellar structure without evidence of phase separation. Importantly, mixing SLM mixed with 30 wt% of formulation A (Fig. 6d) shows a more pronounced alteration of the thermal profile compared to the thermogram of pristine SLM. Indeed, a drastic reduction in peak definition and the shift of the main endothermic event toward lower temperatures indicate strong interaction between [6]-gingerol and the lipid components. In the mixture containing 30 wt% of formulation B (Fig. 6e), the DSC curve becomes even more complex, suggesting further interactions of both actives with the biomimetic lipid matrix.

3.6. Histological distribution in the skin layers of actives from cream formulations

At bright microscopy, no histological modifications were observed in explanted skin between controls and samples treated with the different formulations and maintained in the bioreactor for 6 h (Fig. 7). In fact, both control (CTR T0 and CTRB) and treated samples showed the typical skin structure characterised by an outer layer, the epidermis, and an inner layer, the dermis. In detail, the epidermis showed the outer squamous layer composed of anucleated cells (corneocytes) and the underlying layer composed of keratinocytes at different differentiation stages. In the dermal layer, the upper part of compact connective tissue (papillary dermis), and the deeper looser part (reticular dermis) were clearly recognisable. Finally, the typical introflections of dermis (dermal papillae) and blood vessels belonging to the papillary and reticular capillary plexus were clearly visible. Therefore, no evident morphological modification of the histological architecture or cytological features was observed in human skin during actives permeation, suggesting their widespread distribution rather than an accumulation in skin components.

4. Discussion

It is well documented that ginger exhibits anti-inflammatory effects through the inhibition of lipoxygenase and COX (Al-Radadi et al., 2022; Yeshi et al., 2022), while spilanthol inhibits the production of pro-inflammatory cytokines, which are molecules contributing to inflammation in the body (Huang et al., 2018). The metabolism of [6]-gingerol, however, occurs primarily at the GI and hepatic levels following oral administration, which may limit the systemic bioavailability and effectiveness of this molecule when taken orally. To circumvent this

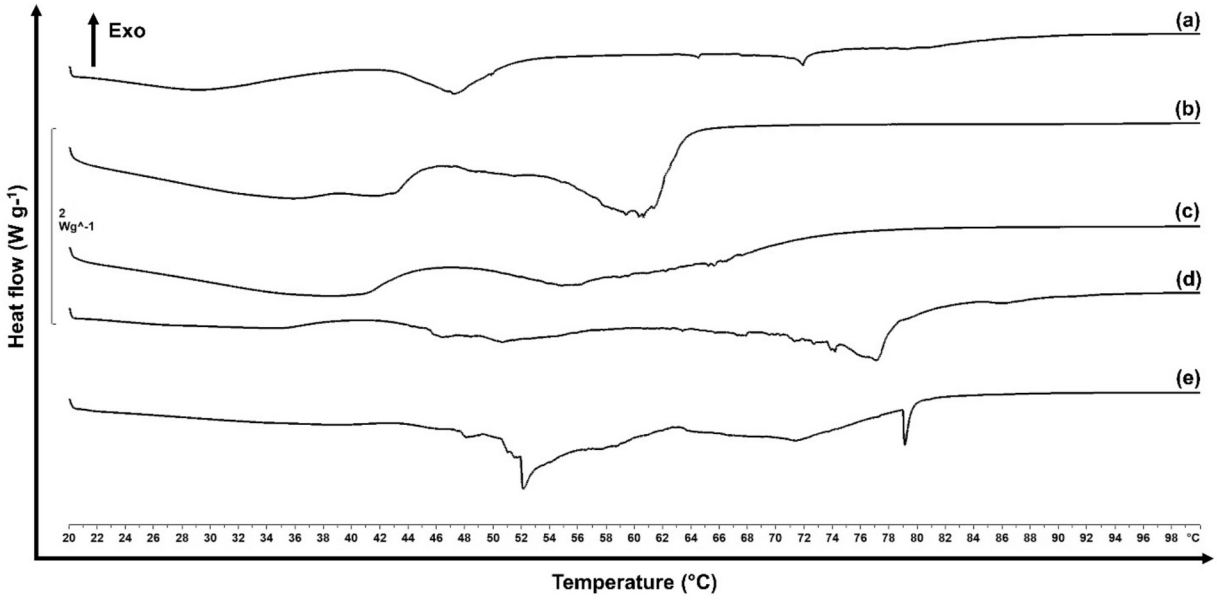

Fig. 6. DSC thermograms of (a) Transdermal vehicle Pentravan®, (b) SLM, (c) mixture of SLM mixed and 30 wt% of transdermal vehicle Pentravan®, (d) mixture SLM and 30 wt% of formulation A and (e) SLM mixed with 30 wt% of formulation B.

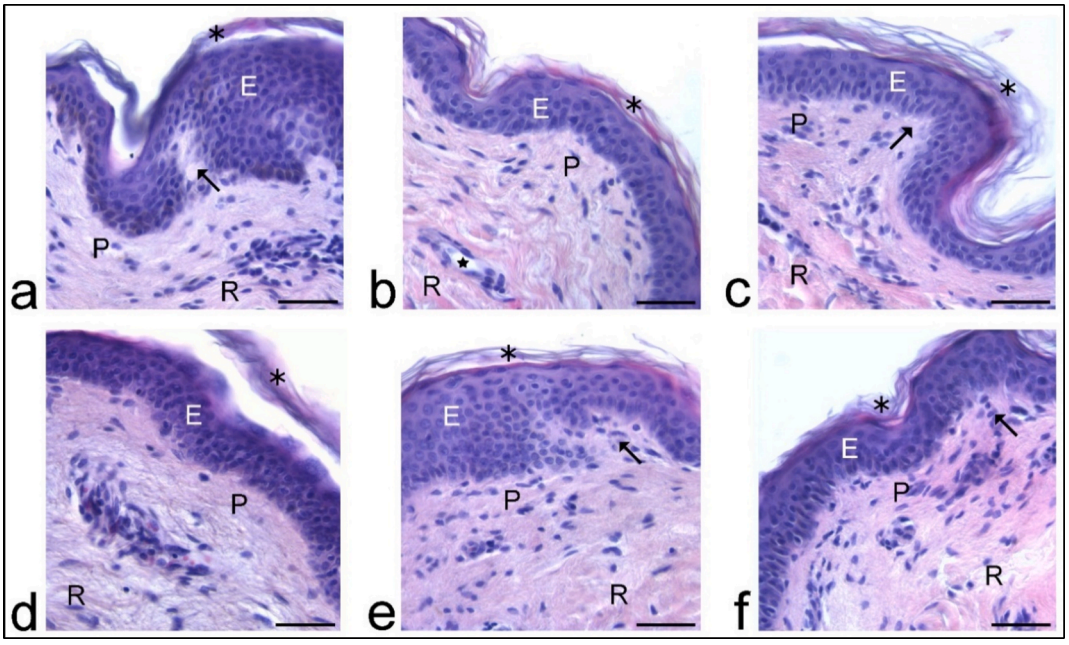

Fig. 7. Light microscopy micrographs of control and treated skin explants (a, CTR T0; b, CTRB; c, Transdermal vehicle; d, Zingiber, e, Acmella; f, Zingiber + Acmella. No modifications are evident. In all samples the epidermis (E) with its corneous layer (asterisks), and the papillary (P) and reticular (R) dermis are visible. Star indicates blood vessels; arrows indicate dermal papillae. Bars: 50 μm.

limitation, the transdermal route presents a promising alternative, as it could facilitate direct delivery to the target site. The application of [6]-gingerol through the skin not only minimises the first-pass metabolism but also offers a more efficient means of achieving therapeutic concentrations at the site of action, potentially improving its clinical efficacy in treating inflammatory conditions. Topical preparations of [6]-gingerol are limited, with two relevant examples regarding the development of proliposomes (Wang, 2018), and a self-microemulsifying delivery system (Xu et al., 2016). Transfersomes (TF), which are deformable liposomes loaded with [6]-gingerol, have also been developed for osteoporosis treatment (Ghazwani et al., 2023). To our knowledge, there are very few published reports on skin permeation of spilanthol loaded in novel vesicular carriers. The study of Afzal et al. (Afzal et al., 2023) reported that herbal emulgels containing Spilanthes acmella exhibits high antibacterial action against dermatitis. The current study, at our knowledge, is the first example presented in the literature showing the combination of these two extracts for a topical application, where the two active compounds may exert their anti-inflammatory properties. In our study, we developed topical formulations through mechanical incorporation of natural extracts into a ready-to-use transdermal vehicle available commercially. Specifically, the commercial base is an oil-in-water emulsion with a liposomal structure that allows the incorporation of high concentrations of both hydrophilic and lipophilic active ingredients. Its composition includes phosphatidylcholine-based liposomes, which are known for their strong affinity to the epidermis. These vesicles can encapsulate compounds in both aqueous and lipid phases, making them particularly suitable for delivering poorly soluble or poorly permeable molecules. Liposomes also mimic biological membranes, facilitating skin interaction and enhancing drug diffusion (Sharma, 1997; Lian, 2001). Moreover, such formulation contains fatty acid esters including isopropyl palmitate and isopropyl myristate, which are well-known penetration enhancers (Nining et al., 2023). These components likely contributed to the high skin permeation of highly lipophilic compounds such as [6]-gingerol and spilanthol, despite their unfavourable thermodynamic profile for passive diffusion through the stratum corneum. Formulation A consisted of *Zingiber officinale* extract mechanically incorporated in the oil-in-water base, while formulation B contained both *Zingiber officinale* and *Acmella oleracea* in the same vehicle. The observed differences in skin permeation between the two formulations may therefore result from a combination of different factors that cannot attributed exclusively to the intrinsic permeability-enhancing properties of the base. Additional factors, including the synergistic or competitive interactions between the active compounds and the vehicle components can play a role on the final permeability enhancement of the actives. The Higuchi model, applied to describe the release kinetics, showed a good linear correlation for all tested formulations, confirming that diffusion is the predominant mechanism governing the release of [6]-gingerol and spilanthol from the topical creams. Notably, the release of [6]-gingerol from formulation B, which also contains spilanthol, exhibited a higher cumulative release and a better fit to the Higuchi model compared to the data obtained from formulation A (Fig. 3). However, the higher release of [6]-gingerol from formulation B should be interpreted by considering multiple contributing factors. In addition to the presence of spilanthol, which is known to act as a natural permeation enhancer, formulation B exhibited lower viscosity and a softer rheological profile compared to formulation A, suggesting a less structured matrix that can further promote the release of the active compound. It should also be noted that the release experiments were performed using a synthetic dialysis membrane, which does not fully replicate the barrier properties of human skin. Therefore, the observed differences in release between the two formulations cannot be attributed to a single factor but rather to the combined effects of formulation composition and rheological behaviour. In parallel, the release of spilanthol from formulation B also showed strong linearity (Fig. 3), reinforcing the idea that both actives are released via Fickian diffusion mechanisms. These differences are possibly linked to the interplay between the active ingredients and the vehicle. Spilanthol, which is structurally characterised by a lipophilic alkylamide chain, is known to act as a natural permeation enhancer, capable of modulating skin barrier properties and altering membrane fluidity (De Spiegeleer, 2013). The presence of this molecule in the formulation B can facilitate the diffusion of [6]-gingerol possibly through an increase of the amount of solubilized active in the vehicle and/or by modifying the vehicle-membrane interface. Moreover, this synergistic effect suggests that the design of a formulation containing various bioactive components should consider not only the pharmacological activity of individual compounds, but also

their functional roles in modulating release and permeation. The improved release profile of [6]-gingerol in the presence of spilanthol supports the hypothesis of complementary formulation behaviour, which could be leveraged to optimize topical delivery systems. Overall, these findings emphasize the importance of a kinetic analysis to understand the formulation-dependent dynamics of release, and highlight how subtle changes in the composition can significantly impact the bioavailability and performance of natural actives in topical systems. These data are in line with the *ex vivo* permeation study. In addition to penetration-enhancing effects, formulation-dependent physical and rheological properties can also possibly contribute to skin permeation. Both formulation A and B were macroscopically homogeneous, showed no visible phase separation, and remained physically stable for at least 30 days. Although the same oil-in-water base was used, a slight difference in viscosity was detected between formulation A and formulation B. Since diffusion from semisolid matrices is strongly influenced by internal microstructure and resistance to molecular diffusion imposed by the formulation network, even modest variations in viscosity or structural organization can affect the mobility of active compounds thereby their release kinetics. This interpretation is supported by literature reporting an inverse correlation between viscosity and drug release in ointments, creams, emulsions and hydrogels, when other parameters (e.g. solubility and distribution) remain constant (Erös et al., 1994). Similarly, recent studies revealed that changes in rheological properties and microstructure, for instance during application and evaporation ("in-use metamorphosis"), can modulate permeability and drug flux through the skin (Jin et al., 1707). We can therefore speculate that, the differences observed in the release and permeation profiles of the tested formulations can be reasonably attributed to a combined effect of physicochemical interactions involving the two plant extracts and formulation-dependent structural properties of the semisolid matrix. Our results demonstrated that a significantly higher amount of [6]-gingerol permeated through porcine skin in formulation B compared to those observed in formulation A (control cream) ($p = 0.001$) (Table 4; Fig. 4). In addition, also the content of [6]-gingerol retained into the skin in formulation B was significantly higher than those registered for formulation A (Table 5). This can be justified by the presence of *Acmella oleracea* lipophilic extract in such formulation, where spilanthol (the main active in the extract) acts as a skin penetration enhancer (De Spiegeleer, 2013). Previous studies have demonstrated that in the uppermost skin layers, spilanthol shows its penetration enhancing effect (De Spiegeleer, 2013), it can be hypothesized that spilanthol interacts with the lipids of the SC, probably through the insertion of its lipid chain in the structure of *stratum corneum* lipid molecules. This leads to an increased fluidity and a disorder of this layer, which facilitates the penetration of substances (De Spiegeleer, 2013). To further investigate the distribution of the active compounds and standardise their quantification across the SC, we implemented a layer-by-layer analysis using the tape stripping technique. Each individual strip was weighed and the content of [6]-gingerol and spilanthol was normalized to the corresponding strip weight. This approach reduced inter-sample variability and enabled a direct comparison of compound accumulation across SC layers. The strip-by-strip analysis of skin penetration revealed that spilanthol accumulates predominantly in the uppermost SC layers (strips 1–3), whereas [6]-gingerol is found at higher concentrations in deeper strips (6–7) (Fig. 5). This observation further supports the proposed role of spilanthol as a penetration enhancer, potentially by modifying the organisation of the superficial lipid domains and facilitating the diffusion of [6]-gingerol into deeper skin layers. In addition, the higher retention of [6]-gingerol in the E + D can possibly be explained by considering its moderate lipophilicity and amphiphilic character, which likely promote diffusion through the intercellular lipid pathway of the SC and preferential partitioning into the hydrated viable skin layers. This hypothesis has been already confirmed in other published studies for a series phenolic compounds delivered from topical emulsions (Zillich, 2013; Oliveira et al., 2022). Differences in the diffusion kinetics of the two actives can be also influenced by their physicochemical properties and their interactions with the complex cream vehicle. Notably, [6]-gingerol tends to accumulate more in the viable epidermis and dermis, whereas spilanthol shows a more uniform distribution between SC and deeper layers. Overall, these observations suggest that both the physicochemical characteristics of the actives and their interactions with the formulation matrix are key factors influencing skin penetration. These results highlight the importance of normalization in tape stripping protocols and aligns with the strategies for improving the interpretability of skin penetration studies proposed by Guy et al (Maciel Tabosa, 2023). Furthermore, [6]-gingerol from formulation A produced a higher amount of active permeated in the receptor fluid, as well as higher values of flux than those registered for spilanthol from formulation B. This phenomenon can be attributed to differences in chemical structure of the two molecules, and to the presence of several unsaturated groups in spilanthol increases its lipophilicity. This results in a higher partition coefficient of spilanthol (log P = 3.4) compared to [6]-gingerol (log P 2.8 - 3.53), moving further slightly away from the ideal characteristics for skin absorption (log P comprised between 1 and 3) (Vitorino et al., 2015). This higher lipophilicity can partly explain the preferential retention of spilanthol in the superficial skin layers; however, other factors, including molecular weight, structural features, and interactions with the cream matrix, likely also contribute to the observed differences in skin distribution. Moreover, from our data, we can clearly observe that both [6]-gingerol and spilanthol permeated in the receptor fluid after the exposure to topical formulation of *Zingiber officinale* and *Acmella oleracea*. Our results are in line with literature studies which illustrated the ability of [6]-gingerol and spilanthol to penetrate into human skin (Boonen et al., 2010; Minghetti et al., 2007). Additionally, the study of Magnano et al. (Magnano et al., 2022) showed that after exposure to pure ginger extract, the permeability of [6]-gingerol using an artificial barrier namely, SMB (skin-mimicking barrier) is close to permeability data measured through porcine skin. This suggests that the biomimetic barrier may represent an effective alternative to animal model for performing skin penetration experiments. Higher skin permeation observed in formulation B can be also related to the viscosity of such cream, which was lower compared to formulation A (Table 2). While rheological analysis showed that formulation B exhibits lower viscosity and a softer structure compared to formulation A, this alone cannot explain the ~ 3.5-fold increase in [6]-gingerol permeation. Indeed, the slightly lower viscosity of formulation B can be attributed to the presence of N-alkylamides such as spilanthol, which act as internal plasticizers within the semisolid system, weakening intermolecular interactions and slightly modifying the interfacial film formed by emulsifiers, resulting in a less structured system and therefore a reduced viscosity. Similar effects of N-alkylamides and plant-derived lipophilic compounds on the microstructure and rheology of topical emulsions have been reported in the literature (De Spiegeleer et al., 2013; Barbosa et al., 2016; Spinozzi, 2025). The significant permeation enhancement observed for formulation B can rather be explained through a combination of several factors, the main being related to the presence of spilanthol, which acts as a penetration enhancer by modulating lipid organization in the *stratum corneum* and improving the diffusion of [6]-gingerol. Moreover, the enhanced permeation observed for formulation B can increase the local availability of [6]-gingerol in the skin, possibly bringing to an improved biological activity compared to formulation A. Rheological flow properties are critical in predicting how a cream behaves during application: low viscosity at high shear rates corresponds to the condition when the cream is rubbed onto the skin, facilitating spreadability and potential penetration; conversely, high viscosity at low shear rates ensures the product remains stable when at rest, such as in the container or on the palm, preventing it from dripping. This shear-thinning behaviour, observed in both formulations, is a desirable characteristic for topical products (Ali, 2022). The reported high zero-shear viscosities, particularly for formulation A, reflect the theoretical zero-shear condition extrapolated using the Cross model at very low shear

rates ($\dot{\gamma} \approx 0.0003\ s^{-1}$). Specifically, product behavior during storage and application occurs at higher shear rates (0.01–100 s^{-1}), where the viscosities of the formulations decrease significantly to 505 Pa·s for formulation A and 695 Pa·s for formulation B. These values are within the range reported in the literature for standard topical creams (Manian et al., 2022; Moldovan et al., 2017; Drakalska Sersemova et al., 2024); confirming that the formulations exhibit rheological properties consistent with commonly used topical systems. From a practical perspective, the lower viscosity and softer rheological profile of formulation B can possibly be translated into improved spreadability, therefore facilitated application on the skin, which are key factors influencing user comfort and patient compliance. The frequency sweep test further characterizes the viscoelastic behaviour of the formulations by measuring the storage modulus (G') and the loss modulus (G"). Prior to this, the linear viscoelastic region (LVR) was determined to ensure that the applied stress did not irreversibly alter the sample structure. A constant stress of 0.05 Pa was selected within the LVR for the frequency sweep. In this context, G' represents the elastic (stored) energy, while G" reflects the viscous (dissipated) energy. Both moduli increased with frequency, and G' consistently exceeded G" across the tested range, indicating a predominantly elastic, gel-like behaviour. This weak gel structure is advantageous for topical formulations, as it contributes to product stability and controlled release of active ingredients (). At higher frequencies—mimicking faster movements during application formulation A exhibited higher G' and G" values, indicating greater rigidity. In contrast, formulation B showed lower moduli, consistent with its lower viscosity and easier spreadability. At lower frequencies, both formulations behaved similarly, suggesting comparable structural integrity under minimal stress. These rheological differences are relevant to skin permeation. Literature reports have shown that diffusion of the model drug out of the formulation and into the skin might have been hindered by the high viscosity of the systems and thus resulted in a limited total penetration depth (Binder et al., 2019). Therefore, the lower viscosity and elastic modulus of formulation B may contribute to the enhanced permeation of [6]-gingerol observed in our study.

The morphological analysis of human skin explants treated with creams containing either or both *Zingiber officinale* and *Acmella oleracea* extracts did not reveal histological or cytological modification suggestive of accumulation sites or preferential permeation routes, suggesting that the transdermal penetration of actives occurs by physiological diffusion through the tissue (Fig. 7). The topical product both lipophilic extracts, therefore, can represent an interesting alternative dosage form compared to oral formulations. Finally, thanks to the simple method of preparation, it can be realized extemporarily as a galenic formulation.

5. Conclusion

Our findings demonstrated that the new topical formulation containing both *Zingiber officinale* and *Acmella oleracea* extracts can be a promising vehicle to deliver active compounds such as [6]-gingerol and spilanthol for topical treatment. The transdermal vehicle in which the actives were incorporated contains specific ingredients that may positively affect skin permeation without causing tissue damage. Additionally, it was observed that the presence of *Acmella oleracea* lipophilic extract in such formulation promoted the permeation of [6]-gingerol, possibly due to the spilanthol and other N-alkylamides acting as skin penetration enhancers. Although further studies are needed, including *in vivo* investigations, the topical cream containing tboth *Zingiber officinale* and *Acmella oleracea* extracts, which are known for their potential synergistic anti-inflammatory effects, can represent an effective alternative to traditional oral formulations.

Funding support

The authors have no relevant financial disclosures.

CRediT authorship contribution statement

Greta Camilla Magnano: Writing – review & editing, Writing – original draft, Investigation, Data curation, Conceptualization. **Martina Glerean:** Writing – original draft, Investigation, Data curation. **Stefano Dall'Acqua:** Investigation. **Michela Abrami:** Investigation. **Francesca Larese Filon:** Resources, Funding acquisition. **Flavia Carton:** Writing – review & editing, Investigation, Data curation. **Manuela Malatesta:** Writing – review & editing, Supervision, Resources. **Laura Calderan:** Writing – review & editing, Supervision, Resources. **Andrea Galvan:** Writing – review & editing, Investigation. **Dario Voinovich:** Writing – review & editing, Supervision. **Dritan Hasa:** Writing – review & editing, Conceptualization.

Declaration of competing interest

The authors have no known competing financial interests or personal relationships that could have appeared to influence the work reported in this paper.

Appendix A. Supplementary data

Supplementary data to this article can be found online at https://doi.org/10.1016/j.ijpharm.2026.126745.

Data availability

Data will be made available on request.

The data that support the findings of this study are available from the corresponding author upon reasonable request.

References

Rondanelli, M., et al., 2020. Acmella oleracea for pain management. Fitoterapia 140, 104419.

Abdul Rahim, R., et al., 2021. Potential antioxidant and anti-inflammatory effects of spilanthes acmella and its health beneficial effects: a review. IJERPH 18 (7), 3532. https://doi.org/10.3390/ijerph18073532.

Huang, W.-C., Wu, L.-Y., Hu, S., Wu, S.-J., 2018. Spilanthol inhibits COX-2 and ICAM-1 expression via suppression of NF-κB and MAPK signaling in interleukin-1β-stimulated human lung epithelial cells. Inflammation 41 (5), 1934–1944. https://doi.org/10.1007/s10753-018-0837-0.

Ratnasooriya, W.D., Pieris, K.P.P., Samaratunga, U., Jayakody, J.R.A.C., 2004. Diuretic activity of Spilanthes acmella flowers in rats. J. Ethnopharmacol. 91 (2), 317–320. https://doi.org/10.1016/j.jep.2004.01.006.

Molina-Torres, J., Salazar-Cabrera, C.J., Armenta-Salinas, C., Ramírez-Chávez, E., 2004. Fungistatic and bacteriostatic activities of alkamides from Heliopsis longipes roots: affinin and reduced amides. J. Agric. Food Chem. 52 (15), 4700–4704.

Rios, M.Y., Aguilar-Guadarrama, A.B., Gutiérrez, M.del.C., 2007. Analgesic activity of affinin, an alkamide from Heliopsis longipes (Compositae). J. Ethnopharmacol. 110 (2), 364–367. https://doi.org/10.1016/j.jep.2006.09.041.

Boonen, J., Baert, B., Burvenich, C., Blondeel, P., Saeger, S., De Spiegeleer, B., 2010. LC-MS profiling of N-alkylamides in Spilanthes acmella extract and the transmucosal behaviour of its main bio-active spilanthol. J. Pharm. Biomed. Anal. 53, 243–249. https://doi.org/10.1016/j.jpba.2010.02.010.

Huang, C.-H., Chang, L.-C., Hu, S., Hsiao, C.-Y., Wu, S.-J., 2018. Spilanthol inhibits TNF-α-induced ICAM-1 expression and pro-inflammatory responses by inducing heme oxygenase-1 expression and suppressing pJNK in HaCaT keratinocytes. Mol. Med. Rep. 18 (3), 2987–2994.

Semwal, R.B., Semwal, D.K., Combrinck, S., Viljoen, A.M., 2015. Gingerols and shogaols: important nutraceutical principles from ginger. *Phytochemistry*. 117, 554–568.

Arcusa, R., Villaño, D., Marhuenda, J., Cano, M., Cerdà, B., Zafrilla, P., 2022. Potential role of ginger (*Zingiber officinale* Roscoe) in the prevention of neurodegenerative diseases. Front. Nutr. 9. https://doi.org/10.3389/fnut.2022.809621.

Boonen, J., Baert, B., Roche, N., Burvenich, C., De Spiegeleer, B., 2010. Transdermal behaviour of the N-alkylamide spilanthol (affinin) from Spilanthes acmella (Compositae) extracts. J. Ethnopharmacol. 127 (1), 77–84. https://doi.org/10.1016/j.jep.2009.09.046.

Minghetti, P., et al., 2007. Evaluation of the topical anti-inflammatory activity of ginger dry extracts from solutions and plasters. Planta Med. 73 (15), 15. https://doi.org/10.1055/s-2007-993741.

Bouwstra, J.A., Nădăban, A., Bras, W., McCabe, C., Bunge, A., Gooris, G.S., 2023. The skin barrier: an extraordinary interface with an exceptional lipid organization. Prog. Lipid Res. 92, 101252. https://doi.org/10.1016/j.plipres.2023.101252.

Uche, L.E., Gooris, G.S., Bouwstra, J.A., Beddoes, C.M., 2021. Increased levels of short-chain ceramides modify the lipid organization and reduce the lipid barrier of skin

model membranes. Langmuir 37 (31), 9478–9489. https://doi.org/10.1021/acs.langmuir.1c01295.
Uche, L.E., Gooris, G.S., Beddoes, C.M., Bouwstra, J.A., 2019. New insight into phase behavior and permeability of skin lipid models based on sphingosine and phytosphingosine ceramides. Biochim. Biophys. Acta Biomembr. 1861 (7), 1317–1328. https://doi.org/10.1016/j.bbamem.2019.04.005.
Bouwstra, J., 2003. Structure of the skin barrier and its modulation by vesicular formulations. Prog. Lipid Res. 42 (1), 1. https://doi.org/10.1016/S0163-7827(02)00028-0.
Rondanelli, M., et al., 2020. The use of a new food-grade lecithin formulation of highly standardized ginger (*Zingiber officinale*) and acmella oleracea extracts for the treatment of pain and inflammation in a group of subjects with moderate knee osteoarthritis. J. Pain Res. 13, 761–770. https://doi.org/10.2147/JPR.S214488.
Moldovan, M., Lahmar, A., Bogdan, C., Părăuan, S., Tomuță, I., Crișan, M., 2016. Formulation and evaluation of a water-in-oil cream containing herbal active ingredients and ferulic acid. Clujul Medical. 90. https://doi.org/10.15386/cjmed-668.
Matchimabura, N., Praparatana, R., Issarachot, O., Oungbho, K., Wiwattanapatapee, R., 2024. Development of raft-forming liquid formulations loaded with ginger extract-solid dispersion for treatment of gastric ulceration. Heliyon 10 (11). https://doi.org/10.1016/j.heliyon.2024.e31803.
Kerdsakundee, N., Mahattanadul, S., Wiwattanapatapee, R., 2015. Development and evaluation of gastroretentive raft forming systems incorporating curcumin-Eudragit® EPO solid dispersions for gastric ulcer treatment. Eur. J. Pharm. Biopharm. 94, 513–520. https://doi.org/10.1016/j.ejpb.2015.06.024.
Magnano, G.C., et al., 2024. 3D human foreskin model for testing topical formulations of sildenafil citrate. Int. J. Pharm. 649, 123612.
Novianti. Physical Evaluation Of Red Ginger Extract (Zingiber Officinale Rosc.Var. Rubrum)Cream Of 10% And 20% Concentration To Reduce Low Back Pain For Pregnant Women In Second And Third Of Trimesters. Vol. Vol 14, Special Issue 1, 2022, 2022.
Barbero, A.M., Frasch, H.F., 2009. Pig and guinea pig skin as surrogates for human in vitro penetration studies: a quantitative review. Toxicol. In Vitro 23 (1), 1–13. https://doi.org/10.1016/j.tiv.2008.10.008.
Simon, G.A., Maibach, H.I., 2000. The pig as an experimental animal model of percutaneous permeation in man: qualitative and quantitative observations – an overview. Skin Pharmacol. Physiol. 13 (5), 229–234. https://doi.org/10.1159/000029928.
Schmook, F.P., Meingassner, J.G., Billich, A., 2001. Comparison of human skin or epidermis models with human and animal skin in in-vitro percutaneous absorption. Int. J. Pharm. 215 (1–2), 51–56. https://doi.org/10.1016/S0378-5173(00)00665-7.
Wester, R.C., Melendres, J., Sedik, L., Maibach, H., Riviere, J.E., 1998. Percutaneous absorption of salicylic acid, theophylline, 2,4-dimethylamine, diethyl hexyl phthalic acid, andp-aminobenzoic acid in the isolated perfused porcine skin flap compared to manin vivo. Toxicol. Appl. Pharmacol. 151 (1), 159–165. https://doi.org/10.1006/taap.1998.8434.
Magnano, G.C., et al., 2022. Validation and testing of a new artificial biomimetic barrier for estimation of transdermal drug absorption. Int. J. Pharm. 628. https://doi.org/10.1016/j.ijpharm.2022.122266.
« Guidance Document For The Conduct Of Skin Absorption Studies Oecd Series On Testing And Assessment Number 28 ». [En Ligne]. Disponible Sur: Https://One.Oecd.Org/Document/Env/Jm/Mono(2004)2/En/Pdf.
Magnano, G.C., Marussi, G., Larese Filon, F., Crosera, M., Bovenzi, M., Adami, G., 2022. Transdermal permeation of inorganic cerium salts in intact human skin. Toxicol. In Vitro 82. https://doi.org/10.1016/j.tiv.2022.105381.
Guth, K., Schäfer-Korting, M., Fabian, E., Landsiedel, R., Van Ravenzwaay, B., 2015. Suitability of skin integrity tests for dermal absorption studies in vitro. Toxicol. In Vitro 29 (1), 113–123. https://doi.org/10.1016/j.tiv.2014.09.007.
OECD, *Guidance Document for the Conduct of Skin Absorption Studies*. in OECD Series on Testing and Assessment. OECD, 2004. doi: 10.1787/9789264078796-en.
Intawong, S., Kaewiad, K., Muangman, T., Kriangkrai, W., 2025. Enhancing skin permeation of Phlai oil and ginger extracts through lipid nanoparticle encapsulation for anti-inflammatory topical products. BMC Complement Med Ther. 25 (1), 196. https://doi.org/10.1186/s12906-025-04932-9.
Lehman, P.A., 2014. A simplified approach for estimating skin permeation parameters from in vitro finite dose absorption studies. J. Pharm. Sci. 103 (12), 4048–4057. https://doi.org/10.1002/jps.24189.
Goh, C.F., Hadgraft, J., Lane, M.E., 2022. Thermal analysis of mammalian stratum corneum using differential scanning calorimetry for advancing skin research and drug delivery. Int. J. Pharm. 614, 121447. https://doi.org/10.1016/j.ijpharm.2021.121447.
Galvan, A., et al., 2023. An innovative fluid dynamic system to model inflammation in human skin explants. IJMS 24 (7), 6284. https://doi.org/10.3390/ijms24076284.
Calderan, L., et al., 2022. An ex vivo experimental system to track fluorescent nanoparticles inside skeletal muscle. Eur. J. Histochem. 67 (1), déc. https://doi.org/10.4081/ejh.2023.3596.
Cappellozza, E., et al., 2022. A spectrofluorometric analysis to evaluate transcutaneous biodistribution of fluorescent nanoparticulate gel formulations. Eur. J. Histochem. 66 (1). https://doi.org/10.4081/ejh.2022.3321.
Cappellozza, E., Zanzoni, S., Malatesta, M., Calderan, L., 2021. Integrated microscopy and metabolomics to test an innovative fluid dynamic system for skin explants in vitro. Microsc. Microanal. 27 (4), 923–934. https://doi.org/10.1017/S1431927621012010.
Esposito, E., et al., 2022. Ex vivo evaluation of ethosomes and transethosomes applied on human skin: a comparative study. IJMS 23 (23), 15112. https://doi.org/10.3390/ijms232315112.
Cross, M.M., 1965. Rheology of non-newtonian fluids: a new flow equation for pseudoplastic systems. J. Colloid Sci. 20 (5), 417–437. https://doi.org/10.1016/0095-8522(65)90022-X.
Razi, S.M., Motamedzadegan, A., Shahidi, S.-A., Rashidinejad, A., 2020. Steady and dynamic shear rheology as a toolfor evaluation of the interactions between egg white albumin and basil seed gum. Rheol. Acta 59 (5), 317–331. https://doi.org/10.1007/s00397-020-01198-5.
Kanfer, I., Rath, S., Purazi, P., Mudyahoto, N.A., 2017. In vitro release testing of semi-solid dosage forms. Dissolution Technol. 24 (3), 52–60. https://doi.org/10.14227/DT240317P52.
Al-Radadi, N.S., et al., 2022. *Zingiber officinale* driven bioproduction of ZnO nanoparticles and their anti-inflammatory, anti-diabetic, anti-Alzheimer, anti-oxidant, and anti-microbial applications. Inorg. Chem. Commun. 140. https://doi.org/10.1016/j.inoche.2022.109274.
Yeshi, K., Turpin, G., Jamtsho, T., Wangchuk, P., 2022. Indigenous uses, phytochemical analysis, and anti-inflammatory properties of australian tropical medicinal plants. Molecules 27 (12), 3849. https://doi.org/10.3390/molecules27123849.
Wang, Q., et al., 2018. A novel formulation of [6]-gingerol: proliposomes with enhanced oral bioavailability and antitumor effect. Int. J. Pharm. 535 (1–2), 308–315. https://doi.org/10.1016/j.ijpharm.2017.11.006.
Xu, Y., et al., 2016. Enhanced oral bioavailability of [6]-gingerol-SMEDDS: preparation, in vitro and in vivo evaluation. J. Funct. Foods 27, 703–710. https://doi.org/10.1016/j.jff.2016.10.007.
Ghazwani, M., Alqarni, M.H., Hani, U., Alam, A., 2023. QbD-optimized, phospholipid-based elastic nanovesicles for the effective delivery of 6-gingerol: a promising topical option for pain-related disorders. IJMS 24 (12), 9983. https://doi.org/10.3390/ijms24129983.
Afzal, A., et al., 2023. Spilanthes acmella extract-based natural oils loaded emulgel for anti-microbial action against dermatitis. Gels 9 (10), 832. https://doi.org/10.3390/gels9100832.
Sharma, A., 1997. Liposomes in drug delivery: progress and limitations. Int. J. Pharm. 154 (2), 123–140. https://doi.org/10.1016/S0378-5173(97)00135-X.
Lian, T., Ho, R.J.Y., 2001. Trends and developments in liposome drug delivery systems. J. Pharm. Sci. 90 (6), 667–680. https://doi.org/10.1002/jps.1023.
N. Nining, A. Amalia, N. Maharani, et S. Adawiyah. Effect of Isopropyl Myristate and Oleic Acid as the Penetration Enhancer on Transdermal Patch: Characteristics and In-Vitro Diffusion. *Egypt. J. Chem.*. 0(0), p. 0-0, mars 2023, doi: 10.21608/ejchem.2023.180955.7396.
De Spiegeleer, B., et al., 2013. Skin penetration enhancing properties of the plant N-alkylamide spilanthol. J. Ethnopharmacol. 148, avr. https://doi.org/10.1016/j.jep.2013.03.076.
Erös, I., Soósné-Csányi, E., Selmeczi, B., 1994. Influence of viscosity on drug release from ointments, creams, gels and emulsions. Acta Pharm. Hung. 64 (2), 57–61.
Jin, X., Alavi, S.E., Shafiee, A., Leite-Silva, V.R., Khosrotehrani, K., Mohammed, Y., 2023. Metamorphosis of topical semisolid products—understanding the role of rheological properties in drug permeation under the "in use" condition. Pharmaceutics 15 (6), 1707. https://doi.org/10.3390/pharmaceutics15061707.
Zillich, O.V., Schweiggert-Weisz, U., Hasenkopf, K., Eisner, P., Kerscher, M., 2013. Release and in vitro skin permeation of polyphenols from cosmetic emulsions. Intern J of Cosmetic Sci. 35 (5), 491–501. https://doi.org/10.1111/ics.12072.
Oliveira, A.L.S., Valente, D., Moreira, H.R., Pintado, M., Costa, P., 2022. Effect of squalane-based emulsion on polyphenols skin penetration: ex vivo skin study. Colloids Surf. B Biointerfaces 218. https://doi.org/10.1016/j.colsurfb.2022.112779.
Maciel Tabosa, M.A., et al., 2023. Quantification of chemical uptake into the skin by vibrational spectroscopies and stratum corneum sampling. Mol. Pharm. 20 (5), 2527–2535. https://doi.org/10.1021/acs.molpharmaceut.2c01109.
Vitorino, C., Sousa, J., Pais, A., 2015. Overcoming the skin permeation barrier: challenges and opportunities. Curr. Pharm. Des. 21 (20), 2698–2712.
De Spiegeleer, B., et al., 2013. Skin penetration enhancing properties of the plant N-alkylamide spilanthol. J. Ethnopharmacol. 148 (1), 117–125. https://doi.org/10.1016/j.jep.2013.03.076.
Barbosa, A.F., De Carvalho, M.G., Smith, R.E., Sabaa-Srur, A.U.O., 2016. Spilanthol: occurrence, extraction, chemistry and biological activities. Rev. Bras 26 (1), 128–133. https://doi.org/10.1016/j.bjp.2015.07.024.
Spinozzi, E., et al., 2025. Hydrogels powered by nanoemulsion technology for the topical delivery of acmella oleracea extract. Pharmaceutics 17 (5), 625. https://doi.org/10.3390/pharmaceutics17050625.
Ali, A., et al., 2022. Relationship between sensorial and physical characteristics of topical creams: a comparative study on effects of excipients. Int. J. Pharm. 613, 121370. https://doi.org/10.1016/j.ijpharm.2021.121370.
Manian, M., Jain, P., Vora, D., Banga, A.K., 2022. Formulation and evaluation of the in vitro performance of topical dermatological products containing diclofenac sodium. Pharmaceutics 14 (9), 1892. https://doi.org/10.3390/pharmaceutics14091892.
Moldovan, M., Lahmar, A., Bogdan, C., Părăuan, S., Tomuță, I., Crișan, M., 2017. Formulation and evaluation of a water-in-oil cream containing herbal active ingredients and ferulic acid. Medicine and Pharmacy Reports. 90 (2), 212–219. https://doi.org/10.15386/cjmed-668.
Drakalska Sersemova, E., et al., 2024. Preparation and characterization of amphiphilic cream formulations with meloxicam. PHAR 71, 1–7. https://doi.org/10.3897/pharmacia.71.e139355.
Binder, L., Mazál, J., Petz, R., Klang, V., Valenta, C., 2019. The role of viscosity on skin penetration from cellulose ether-based hydrogels. Skin Res. Technol. 25 (5), 725–734. https://doi.org/10.1111/srt.12709.